

GEOLOGICAL MAPPING IN MOROZUMI RANGE AND HELLIWELL HILLS AREAS, NORTHERN VICTORIA LAND (NVL), ANTARCTICA USING REMOTE SENSING IMAGERY

Amin Beiranvand Pour^{1,2}, Yongcheol Park¹, Jong Kuk Hong¹, Aidy M Muslim and Biswajeet Pradhan³

¹ Korea Polar Research Institute (KOPRI) Songdomirae-ro, Yeonsu-gu, Incheon 21990, Republic of Korea

²Institute of Oceanography and Environment (INOS), Universiti Malaysia Terengganu (UMT), 21030 Kuala Nerus, Terengganu, Malaysia

³School of Systems, Management and Leadership, Faculty of Engineering and Information Technology, University of Technology Sydney, New South Wales, Australia

Email: beiranvand.amin80@gmail.com; ypark@kopri.re.kr; jkhong@kopri.re.kr; aidy@umt.edu.my; Biswajeet.Pradhan@uts.edu.au

KEY WORDS: ASTER; Landsat-8; Inaccessible regions; Geological mapping Independent component analysis (ICA); Constrained Energy Minimization (CEM)

ABSTRACT: Many regions remain poorly studied in terms of geological mapping in inaccessible regions especially in the Arctic and Antarctica due to harsh conditions and logistical difficulties. Application of specialized image processing techniques is capable of revealing the hidden linearly mixed spectral sources in multispectral and hyperspectral satellite images. In this study, the application of Independent component analysis (ICA) and Constrained Energy Minimization (CEM) algorithms was evaluated for Landsat-8 and Advanced Spaceborne Thermal Emission and Reflection Radiometer (ASTER) remote sensing data for geological mapping in Morozumi Range and Helliwell Hills areas, Northern Victoria Land (NVL), Antarctica. ICA algorithm was able to detect hidden linearly mixed spectral sources and low probability target materials in Landsat-8 and ASTER datasets. Fraction images of endmember target minerals such as hematite, goethite, jarosite, alunite, kaolinite, muscovite, epidote, chlorite, calcite, quartz, opal and chalcedony were produced using CEM algorithm for two spatial subsets of ASTER scene covering the Morozumi Range and Helliwell Hills areas. CEM classification image maps indicated that chlorite/hematite, goethite/jarosite/calcite and kaolinite/muscovite are governed in the Morozumi Range and goethite, chlorite, hematite and epidote are most dominated mineral assemblages in the Helliwell Hills area. GPS survey and XRD analysis verified the alteration mineral assemblages detected by ICA and CEM image processing algorithms. The results of this investigation demonstrate the capability of the two algorithms in distinguishing pixel and subpixel targets in the multispectral satellite data. The application of the methods for identifying poorly exposed geologic materials and subpixel exposures of alteration minerals has invaluable implications for geological mapping and mineral exploration in inaccessible regions.

1. INTRODUCTION

Geological investigations in the Arctic and Antarctica confront many difficulties due to their remoteness and extreme environmental conditions. Largely, due to harsh conditions and logistical difficulties, many areas remain poorly studied in terms of geological mapping and mineral exploration point of view. Recently, few studies emphasized the application of remote sensing satellite imagery for geological mapping in the Arctic and Antarctic environments (Pour et al., 2019a,b). Several investigations used the Advanced Spaceborne Thermal Emission and Reflection Radiometer (ASTER), HyMap and Landsat-8 remote sensing data and some conventional and sophisticated image processing techniques to extract geological and mineralogical information in the Sarfartoq carbonatite complex, southern West Greenland, the Kap Simpson complex area, East Greenland, the Graham Land of Antarctic Peninsula, West Antarctica and the Kerr-Sulphurets-Mitchell (KSM) and Snowfield zones in the northwestern British Columbia (Bedini, 2009; Sheikhrhimi et al., 2019; Noori et al., 2019). Results indicate that the implementation of suitable image processing algorithms to multispectral and hyperspectral remote sensing data can increase the possibility of

extracting detailed geological and mineralogical information for remote and inaccessible regions. The highest percentage of exposed rocks and soils in Antarctica occurs along the Transantarctic Mountains (TAM) from the Pacific to the Atlantic side of the continent, especially in Northern Victoria Land (NVL) (Fig. 1), where over 5% of the emerged land is ice-free (Salvi et al., 2001). Rocks now exposed in NVL were part of the over 4000 km long paleo-Pacific margin of East Gondwana during the Paleozoic time (Veevers, 2005). A few multispectral satellite remote sensing investigations have been conducted for geological applications in NVL, Antarctica.

In this investigation, the application of Independent component analysis (ICA) and Constrained Energy Minimization (CEM) algorithms is evaluated for detailed mapping of exposed lithologies and alteration mineral zones in Morozumi Range and Helliwell Hills regions of NVL using Landsat-8 and ASTER remote sensing data. The Morozumi Range and Helliwell Hills regions of NVL were selected for the present study because their exposed lithological units are located in remote and inaccessible zone (between Gressitt and Rennick Glaciers of the NVL) (Fig. 1). Moreover, geological fieldwork information for these regions were collected during 2015-2016 summer season expeditions by Korea Polar Research Institute (KOPRI), which could be used for verifying the results of the image processing algorithms.

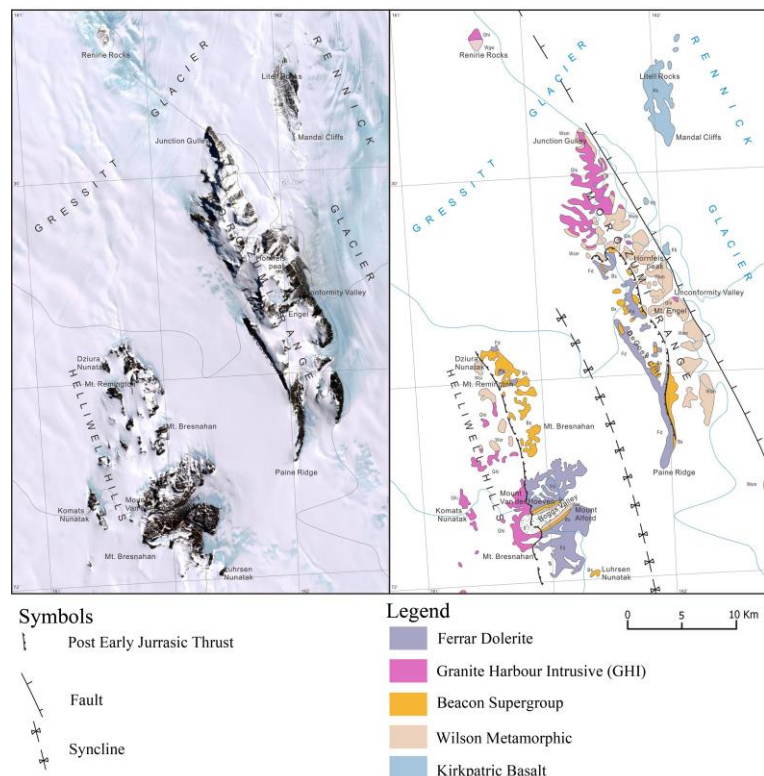


Figure 1. Google Earth image and geology map of the Morozumi Range and Helliwell Hills regions.

2. MATERIALS AND METHODS

2.1 Remote sensing data

In this study, a Landsat-8 level 1T image (LC80671112017038LGN00) (Path/Row 067/111) covering the study area were obtained from the U.S. Geological Survey Earth Resources Observation and Science Center (EROS) (<http://earthexplorer.usgs.gov>). During acquisition date of the image (2017/02/07), sun elevation and azimuth were 24.078 and 62.411, respectively. Scene cloud cover is 4.06 % for the Landsat-8 image. An ASTER level 1T (Precision Terrain Corrected Registered At-Sensor Radiance) scene (AST_L1T_00301022005221353_20150507182028_120722) (Path/Row 068/111) covering the Morozumi Range and Helliwell Hills areas was obtained from U.S. Geological EROS (<http://glovis.usgs.gov/>). It was acquired on January 2, 2005. Sun elevation and azimuth were recorded as 34.665 and 53.756, respectively. Scene cloud cover is 4 % for the ASTER image used in this study. The Landsat-8 and ASTER datasets were processed using the ENVI (Environment for Visualizing Images) version 5.2 and Arc GIS version 10.3 software packages.

2.2 Data analysis

In this analysis, the atmospheric correction was applied to the Landsat-8 and ASTER scenes using Fast Line-of-sight Atmospheric Analysis of Spectral Hypercube (FLAASH) algorithm (Cooley et al., 2002). The FLAASH algorithm was implemented using the Sub-Arctic Summer (SAS) atmospheric and the Maritime aerosol models. ICA is an unsupervised method in the sense that it takes the input data in the form of a single data matrix. It is not necessary to know the desired output of the system or to divide the measurements into different conditions. This is in strong contrast to classical scientific methods based on some experimentally manipulated variables, as formalized in regression or classification methods. ICA is thus an exploratory or data-driven method. It can simply measure some system or phenomenon without designing different experimental conditions. ICA can be used to investigate the structure of the data when suitable hypotheses are not available, or they are considered too constrained or simplistic (Hyvarinen et al., 2001). ICA was applied to Landsat-8 (VNIR+SWIR+TIR bands) and ASTER (VNIR+SWIR and TIR bands) datasets for selected spatial sub-scene of the Morozumi Range and Helliwell Hills. CEM is a target signature-constrained approach, which constrains the desired target signature with a specific gain while minimizing effects caused by other unknown signatures (Jiao and Chang, 2008). This approach was derived from the minimum variance distortionless response (MVDR) in sensor array processing with the desired signature interpreted as the desired direction of signal arrival (Van Veen and Buckley, 1998). To apply the CEM to VNIR+SWIR ASTER data, new covariance statistics were computed. Subspace background was implemented to remove anomalous pixels before calculating background statistics. The fraction of the background in the anomalous image was adjusted by the threshold of 0.750 for the entire image for calculating the subspace background statistics. Covariance matrix method was selected for the calculation.

3. RESULTS AND DISCUSSION

An enhanced red-green-blue (RGB) color combination was assigned to IC3, IC4 and IC7 of Landsat-8 for mapping and discrimination of geologic materials in the study area. The image map provides a color-based classification of the selected subset scene of Landsat-8 (Fig. 2) and shows lithological boundaries and different snow facies efficiently. With reference to geology maps of the study area (see Fig. 1), Ferrar Dolerite appears in magenta color, Granite Harbour Intrusive (GHI) is green to cyan color, Beacon Supergroup and amphibolite facies and metasediment of Wilson metamorphic represent as whitish yellow to yellow color, and topographical shadowing is red in color. The different shades of brown, blue, mustard and purple on the glacier correspond to the different snow facies. It seems that mustard shade in the northeastern part of the Morozumi Range and green shade especially adjacent to exposure of Granite Harbour Intrusive (GHI) in the northern part of the Morozumi are admixtures of snow/ice with very poor exposed lithologies.

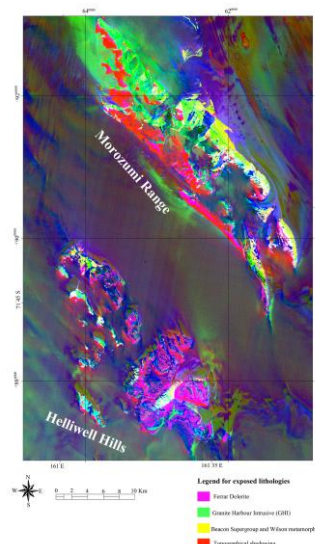


Figure 2. Landsat-8 image map derived from IC3, IC4 and IC7 as RGB color combination for selected spatial subset scene covering the Morozumi Range and Helliwell Hills.

The analysis of statistical factors for VNIR+SWIR ICA components of ASTER shows that maximally independent pixels could be found in IC2, IC6 and IC7. The RGB color combination was produced to visualize anomaly pixels in IC2, IC6 and IC7 components. Figure 3 shows exposed lithological units in the selected subset scene of ASTER covering the Morozumi Range and Helliwell Hills areas. Considering the geological map of the study area, Ferrar

Dolerite represents in whiteish yellow to pearl color, Granite Harbour Intrusive (GHI) is yellow to cyan color, Beacon Supergroup appears in green color and amphibolite facies and metasediment of Wilson metamorphic characterize in blue color pixels. Topographical shadowing was not recorded in the ASTER image map (Fig. 3). Admixtures of snow/ice with very poor exposed lithologies appear as magenta pixels in margins of the exposures. More detailed lithological discrimination was identified in comparison with Landsat-8 resultant image map (see Fig. 2).

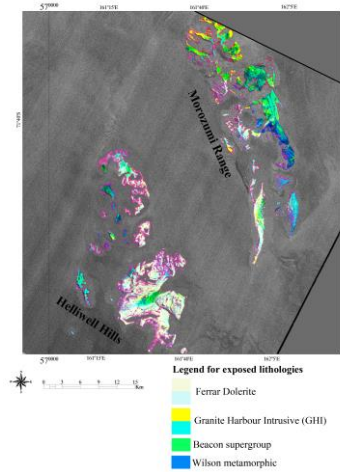


Figure 3. ASTER image map derived from IC2, IC6 and IC7 as RGB color combination for selected spatial subset scene covering the Morozumi Range and Helliwell Hills.

IC2, IC3 and IC4 components were generated using ASTER TIR bands 11, 12 and 13, respectively. An RGB color combination was assigned to IC2, IC3 and IC4 components for discriminating mafic to felsic trend of exposed lithologies in the Morozumi Range and Helliwell Hills areas. Figure 4 displays exposed lithological units in the selected subset scene of ASTER covering the study area. In view of the geological map of the study area (see Fig. 2), Granite Harbour Intrusive (GHI) appears red color (felsic trend), Ferrar Dolerite depicts yellow color (mafic trend), Beacon Supergroup and Wilson metamorphic represent light yellow to magenta color (basic to intermediate trend). Cyan color pixels are poorly exposed lithological units (Fig. 4).

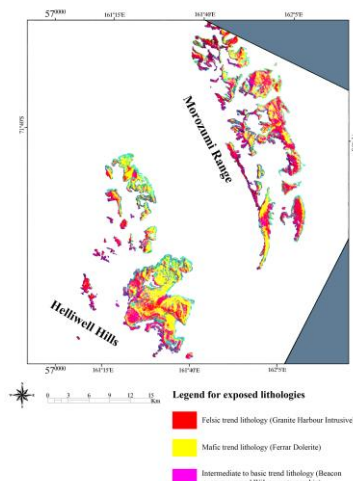


Figure 4. ASTER image map derived from IC2, IC3 and IC4 as RGB color combination for selected spatial subset scene covering the Morozumi Range and Helliwell Hills.

Two spatial subsets of ASTER scene covering the Morozumi Range and Helliwell Hills areas were selected for implementation of the CEM algorithm herein. Fractional abundance of the target endmember minerals was detected using CEM algorithm for the selected zones, separately. Twelve fraction images resulted from this analysis for the selected zones, appear as a series of gray scale rule images, one for each selected endmember. Bright pixels (high Digital Number (DN) value) in each gray scale image show a high fractional abundance of the target mineral. The value in the rule image represents the subpixel abundance of the target mineral in each pixel. Surface distribution of the subpixel abundance related to target minerals appears as high DN value pixels (bright pixels) in the gray scale fraction images. Figure 5 shows CEM classification image map for the Morozumi Range. Some target endmember minerals such as chlorite/hematite, goethite/jarosite/calcite and kaolinite/muscovite are spectrally governed the Morozumi Range and their corresponding fraction images map out the minerals' distribution. Other minerals such as

alunite, epidote, opal, chalcedony and quartz have less contribution in total mixed spectral features of the study zone. CEM classification image map for the Helliwell Hills region is shown in Figure 6. Analysis of the results indicates that goethite, chlorite, hematite and epidote are most dominated mineral assemblages in this zone. Jarosite, muscovite, kaolinite and alunite are shown the second fractional abundance of mineral assemblages, while calcite, opal, chalcedony and quartz have very low surface distribution in the Helliwell Hills region.

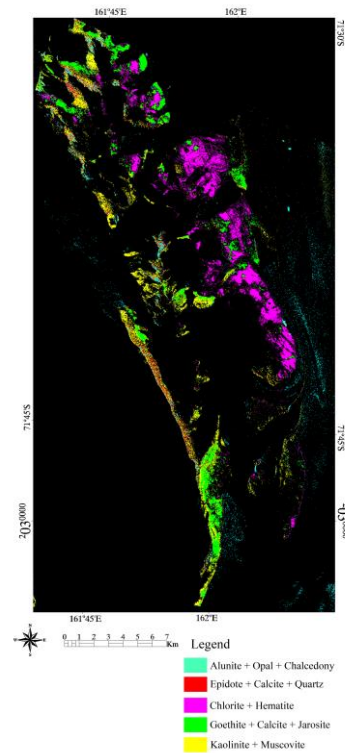


Figure 5. CEM classification image map for the Morozumi Range spatial subset zone.

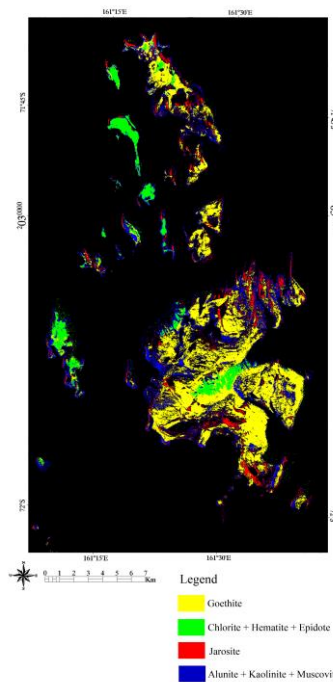


Figure 6. CEM classification image map for the Helliwell Hills spatial subset zone.

4. CONCLUSIONS

The application of Independent component analysis (ICA) and Constrained Energy Minimization (CEM) algorithms was evaluated for detailed mapping of exposed lithologies and alteration mineral zones in Morozumi Range and Helliwell Hills region of NVL using Landsat-8 and ASTER remote sensing data. The results of the investigation demonstrate that these algorithms hold great potential for geological mapping applications and should be of special interest for Polar Earth scientists who might have very limited ground truth, for geologic mapping in areas with significant vegetative cover as well as for mineral exploration by enabling the detection of subpixel exposures of minerals indicative of hydrothermal alteration zones.

Acknowledgements

This study was conducted as a part of KOPRI research grant PE17160. KOPRI grants PE17050 was also acknowledged for supporting the research. We are thankful to Korea Polar Research Institute (KOPRI) for providing all the facilities for this investigation. University Technology Malaysia (UTM) also appreciated.

REFERENCES

- Bedini, E., 2009. Mapping lithology of the Sarfartoq carbonatite complex, southern West Greenland, using HyMap imaging spectrometer data. *Remote Sensing of Environment*, 113, 1208-1219.
- Cooley, T., Anderson, G.P., Felde, G.W., Hoke, M.L., Ratkowski, A.J., Chetwynd, J.H., Gardner, J.A., Adler-Golden, S.M., Matthew, M.W., Berk, A., Bernstein, L.S., Acharya, P.K., Miller, D., Lewis, P., 2002. FLAASH, a MODTRAN4-based atmospheric correction algorithm, its application and validation. *Proceedings of the Geoscience and Remote Sensing Symposium, 2002, IEEE International*, 3, 1414–1418.
- Hyvärinen A. Karhunen, J., Oja, E. 2001. Independent component analysis. A Wiley-Interscience Publication JOHN WILEY & SONS, INC. pp.1-12.
- Jiao, X., and Chang, C.I. 2008. Kernel-Based Constrained Energy Minimization (K-CEM). *Algorithms and Technologies for Multispectral, Hyperspectral, and Ultraspectral Imagery XIV*, edited by Sylvia S. Shen, Paul E. Lewis, *Proc. of SPIE Vol. 6966, 69661S*, (2008) · 0277-786X/08/\$18 · doi: 10.1117/12.782221
- Noori, L., Pour, B.A., Askari, G., Taghipour, N., Pradhan, B., Lee, C-W., Honarmand, M., 2019. Comparison of Different Algorithms to Map Hydrothermal Alteration Zones Using ASTER Remote Sensing Data for Polymetallic Vein-Type Ore Exploration: Toroud–Chahshirin Magmatic Belt (TCMB), North Iran. *Remote Sensing*, 11 (5), 495; doi.org/10.3390/rs11050495.
- Pour, A.B., Hashim, M., Hong, J.K., Park, Y. 2019a. Lithological and alteration mineral mapping in poorly exposed lithologies using Landsat-8 and ASTER satellite data: north-eastern Graham Land, Antarctic Peninsula. *Ore Geology Reviews*, 108, 112-133.
- Pour, A.B., Park, Y., Crispini, L., Läufer, A., Kuk Hong, J., Park, T.-Y.S., Zoheir, B., Pradhan, B., Muslim, A.M., Hossain, M.S., Rahmani, O. 2019b. Mapping Listvenite Occurrences in the Damage Zones of Northern Victoria Land, Antarctica Using ASTER Satellite Remote Sensing Data. *Remote Sensing* 11, 1408. doi.org/10.3390/rs11121408.
- Sheikhrahimi, A., Pour, B.A., Pradhan, B., Zoheir, B., 2019. Mapping hydrothermal alteration zones and lineaments associated with orogenic gold mineralization using ASTER remote sensing data: a case study from the Sanandaj-Sirjan Zone, Iran. *Advances in Space Research* 63, 3315-3332.
- Van Veen., B.D. Buckley, K. M. 1998. Beamforming: a versatile approach to spatial filtering. *IEEE ASSP Mag.* 4–24.